Removal of chromium (VI) from aqueous solutions using *Diospyros discolor* seed activated with nitric acid: isotherm and kinetic studies

Dian Arrisujaya, Nina Ariesta and Mamay Maslahat

ABSTRACT

Diospyros discolor seed activated with nitric acid was investigated for removing Cr(VI) from aqueous solutions. Batch experiments were used to determine the adsorption efficiency, effect of pH, adsorption isotherm, and kinetics. Langmuir and Freundlich adsorption models were used to analyze data of Cr(VI) uptake. Fourier transform infrared spectroscopy was used to investigate the functional groups and surface morphology was checked using a scanning electron microscope, coupled with energy dispersive spectroscopy. The optimum pH in Cr(VI) uptake was 3.5 and the maximum adsorption efficiency reached 100% at 60 min.

Key words | *Diospyros discolor*, seed, hexavalent chromium, isotherm, kinetic parameters, nitric acid

Dian Arrisujaya (corresponding author)
Nina Ariesta
Mamay Maslahat
Department of Chemistry, Faculty of Mathematics and Natural Sciences,
Universitas Nusa Bangsa,
Jl. KH. Sholeh Iskandar Km 4, Bogor 16166,
West Java,
Indonesia
E-mail: *d1anarrisujaya@gmail.com*

INTRODUCTION

Chromium pollution has been related to air and wastewater release of chromium, mainly from metallurgical or natural geology, refractory or industrial activities such as chemical industries, and, potentially, land use (Hausladen *et al.* 2018). There are three kinds of waste from industrial processes: solid, liquid and gaseous. One element contained in liquid waste is the heavy metal chromium(VI) – Cr(VI) – which is hazardous in the environment. River pollution has been the obvious problem. Maximum contaminant level of chromium (total) permitted in drinking water is 0.1 mg/L (U.S. Environmental Protection Agency 2018). There are several methods for reducing Cr(VI) levels in liquid waste, including chemical precipitation, ion exchange, solvent extraction, membrane separation, evaporation, reverse osmosis, and adsorption (Selvaraj *et al.* 2003).

Biosorption research has reported the complexity of the process in terms of physicochemical and biological factors and uncertainty about the mechanisms involved (Fomina & Gadd 2014). Studies of biosorption have focused on isotherms, thermodynamics and the kinetics of interaction. Both batch and continuous methods have been used in biosorption experiments. The batch method enables more interaction between adsorbent and adsorbate than the continuous method. Biosorption has not been commercially successful and its traditional reputation as a low-cost and environmentally friendly pollutant treatment method should be reconsidered (Fomina & Gadd 2014).

Researchers have used different kinds of biological and/or agricultural byproducts for the removal of metal ions, i.e. sugar palm fruit shell (Zein *et al.* 2014); water hyacinth (Rani *et al.* 2017); avocado seed (Murungi & Hassanali 2016); taro (Saha *et al.* 2017); fungi (Garza-González *et al.* 2017); flamboyant pod (Abdel-Rahman *et al.* 2016); pineapple crown leaf (Gogoi *et al.* 2018), etc. Adsorbents produced from natural resources have the main advantages of being sourced from low-cost, easily available materials. Some parts of plants or natural resources have been used to produce adsorbents because they contain functional groups such as hydroxyl, aldehyde, amine, amide and aliphatic acid (Naiya *et al.* 2011).

In general, the two processes in adsorbent activation are physical and chemical activation, to increase the surface area and develop porosity. Acids, bases, and oxidizing agents have been used to activate the adsorbent by producing favorable chemical and physical properties (Chen & Wu 2004). The Chemical process causing the adsorption process is ion exchange, whereas the physical process is through electrostatic forces (Deng *et al.* 2015). Chen & Wu (2004) found that nitric acid generates a large number of surface carbonyl, carboxyl and nitrate groups.

doi: 10.2166/wst.2019.125

Diospyros discolor is a fruit from Bogor, West Java, Indonesia, locally called *bisbul*. It has antidiarrhoeal (Howlader *et al.* 2012) and analgesic properties (Akter *et al.* 2015). Until now, research into the use of the seed as an adsorbent has not been conducted. This paper discusses with the potency of *D. discolor* seed, activated by nitric acid, as the adsorbent for Cr(VI). It also discusses the isotherms and kinetics of adsorption.

METHODS

Materials

D. discolor fruit was bought from the traditional market in Bogor. All reagents used for preparation and analysis were obtained from Merck (Darmstadt, Germany) and used without any further purification: potassium dichromate ($K_2Cr_2O_7$), nitric acid (HNO_3, 65%), hydrochloric acid (HCl, 95%), and ethanol. Cr(VI) working standard solution was prepared from 1,000 mg/L stock standard solution.

D. discolor seed preparation

The cleaned seeds were ground and sieved. The powder was soaked and stirred in ethanol for 2 hours. The next soaking was in HNO_3 0.1 M for 2 hours to activate the sites to act as adsorbents. The resulting adsorbent was dried in an oven at a temperature of 60 °C for 8 hours.

Batch adsorption experiment

A stock solution containing 1,000 mg/L was prepared using potassium dichromate and distilled water. The adsorbent (1 g) was mixed with Cr(VI) solution in 100 mL Erlenmeyer flasks. They were agitated on a shaker at 125 rpm for the relevant amount of time to ensure equilibrium. The controlling parameter of adsorption was determined by varying the pH (2.5, 3, 3.5, 4, and 4.5), the concentration of adsorbate (5, 10, 20, 40, 60, 80 and 100 mg/L), the dosage of adsorbent (10, 20, 30, 40 and 50 g/L) and the contact time (10, 20, 30, 40, 50 and 60 min). Finally, the solution was filtered through filter paper.

The adsorption capacity (q_e) of Cr(VI) was calculated using Equation (1):

$$q_e = \frac{(C_0 - C_e)}{m} \times V \tag{1}$$

The adsorption efficiency (%E) of Cr(VI) was calculated using Equation (2):

$$\%E = \frac{(C_0 - C_e)}{C_0} \times 100\% \tag{2}$$

where C_o and C_e (mg/L) are the Cr(VI) concentrations in the solution before and after the treatment, respectively. V (L) represents the volume of Cr(VI) solution and m (g) is the mass of adsorbent used.

Isotherm and kinetic studies

Isotherm models

The adsorption isotherms models employed to fit the experimental data are shown in Equations (3) and (4).

Langmuir isotherm model:

$$q_e = \frac{q_m\, b\, C_e}{1 + b\, C_e} \tag{3}$$

Freundlich isotherm model:

$$q_e = K_F C_e^{\frac{1}{n}} \tag{4}$$

where q_e is the adsorption capacity (mg/g) at equilibrium; q_m is the maximum adsorption capacity (mg/g); b is the Langmuir adsorption equilibrium constant (L/mg); C_e is the equilibrium concentration of Cr(VI) (mg/L). K_F is the constant related to adsorption capacity in the Freundlich model; n is the constant related to adsorption intensity between the adsorbent and the adsorbate.

Kinetic models

The pseudo-first-order (Lagergren 1898) model, Equation (5), with the linear form shown in Equation (6), describes the rate of sorption to be proportional to the number of sites unoccupied by the solutes.

$$\frac{dq_t}{dt} = k_1(q_e - q_t) \tag{5}$$

$$\log(q_e - q_t) = \log(q_e) - \frac{k_1}{2.303}t \tag{6}$$

The pseudo-second-order (Ho 2006) model, Equation (7), with the linear form shown in Equation (8) works well only in the regions where the biosorption process occurs rapidly.

$$\frac{dq_t}{dt} = k_2(q_e - q_t)^2 \quad (7)$$

$$\frac{t}{q_t} = \left(\frac{1}{k_2 q_e^2}\right) + \left(\frac{1}{q_e}\right)t \quad (8)$$

The Elovich (Chien & Clayton 1980) model, Equation (9), with its linear form shown in (10), describes the kinetics of the chemisorption process:

$$\frac{dq_t}{dt} = \alpha\ exp\ (-\beta q_t) \quad (9)$$

$$q_t = \left(\frac{1}{\beta}\right)\ln(\alpha\beta) + \left(\frac{1}{\beta}\right)\ln t \quad (10)$$

where q_t and q_e are adsorption capacities (mg/g) at any time (t) and at equilibrium (e) respectively, k_1 is the first-order rate constant (min^{-1}), k_2 is the second-order rate constant (g/mg min), α is the initial adsorption rate constant (mg/g min) and β is the Elovich constant (g/mg).

Characterizations

The morphologies of samples were observed on scanning electron microscope (SEM) (ZEISS EVO® MA 10, Carl Zeiss Group, Germany), coupled with energy dispersive spectroscopy (EDS). Structure and interactions were monitored using a Fourier transform infrared (FT-IR) spectrometer (Thermo Nicolet Avatar 360, Nicolet Co., USA). The concentration of Cr(VI) was measured using an atomic absorption spectrometer (AAS) (Agilent 240FS AA, Agilent Co., USA).

RESULTS AND DISCUSSION

Characterization of biosorbent

The FT-IR spectra were analyzed to identify the functional group involved in Cr(VI) adsorption. The FT-IR spectra of *D. discolor* seed are shown in Figure 1. FT-IR spectra of *D. discolor* before and after biosorption were recorded in the wave number range 4,000–500 cm^{-1}. O – H stretch: intermolecular hydrogen bonds, 3,355.97 cm^{-1}. C – H stretch: methylene, 2,940–2,860 cm^{-1}. Overtone or combination bands, 2,000–1,667 cm^{-1}. Normal aldehydic C = O stretch, 1,613.16 cm^{-1}. Aldehydic C – H bend, 1,365.35 cm^{-1}. O – H bend, possibly augmented by C – H in-plane bend, 1,241.45 cm^{-1}. C – O stretch, primary alcohol <1,050 cm^{-1}. The C – C bond is stretched during the contraction of the C – O bond, 950–810 cm^{-1}. Out-of-plane C – H bend, 804.45 cm^{-1} (Naushad *et al.* 2017). The main characteristic of *D. discolor* seed was cellulose, with a peak at 1,000–1,200 cm^{-1} (Abdel-Rahman *et al.* 2016). The shifts in the peak at 3,355.97; 1,613.16; 1,061.72 cm^{-1} indicated binding of Cr(VI) ions to hydroxyl groups, carboxylic acids, and C – O groups respectively. As shown in Figure 1, the increasing percentage of transmittance indicated the absorbance was reduced due to the influence of Cr(VI). A change in intensity and shift in the position of the peaks indicates the involvement of functional groups in the adsorption process (Zein *et al.* 2014).

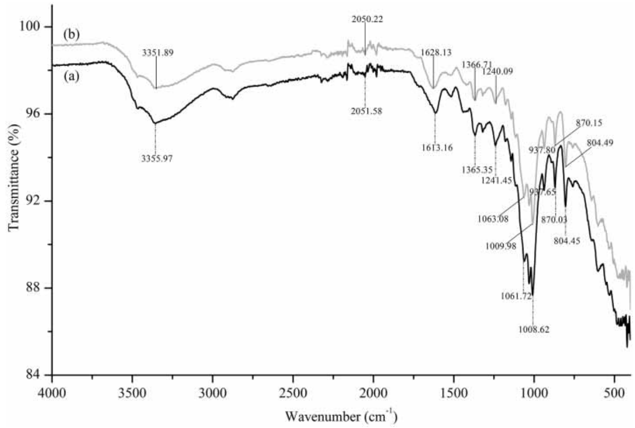

Figure 1 | FT-IR spectra of *D. discolor* seed (a) before and (b) after biosorption.

The surface morphologies of *D. discolor* seed were analyzed by SEM before and after biosorption of Cr(VI) and are shown in Figure 2. The *D. discolor* seed surface before biosorption (Figure 2(a) and 2(b)) show the porosity of the biosorbent: there are many diverse cleavages and pores on the surface. The surface of the biosorbent was covered and the pores became smaller after adsorption of Cr (VI) (Figure 2(c) and 2(d)). There was a clear difference in Figure 2, which was confirmed by calculating the average pore length before adsorption, ±15–39 μm (Figure 2(b)), which became narrower after adsorption, ±2–10 μm (Figure 2(d)).

Elemental analysis of the biosorbent was conducted using EDS. The EDS spectra before and after biosorption of Cr(VI) are shown in Figure 3. There was no peak of chromium in the EDS analysis of *D. discolor* seed before adsorption (Figure 3(a)). However, there was a peak of chromium observed at 5.4 keV (Figure 3(b)). The biosorption of Cr(VI) was confirmed by EDS in *D. discolor* seed activated with nitric acid. The EDS spectra showed a chromium peak

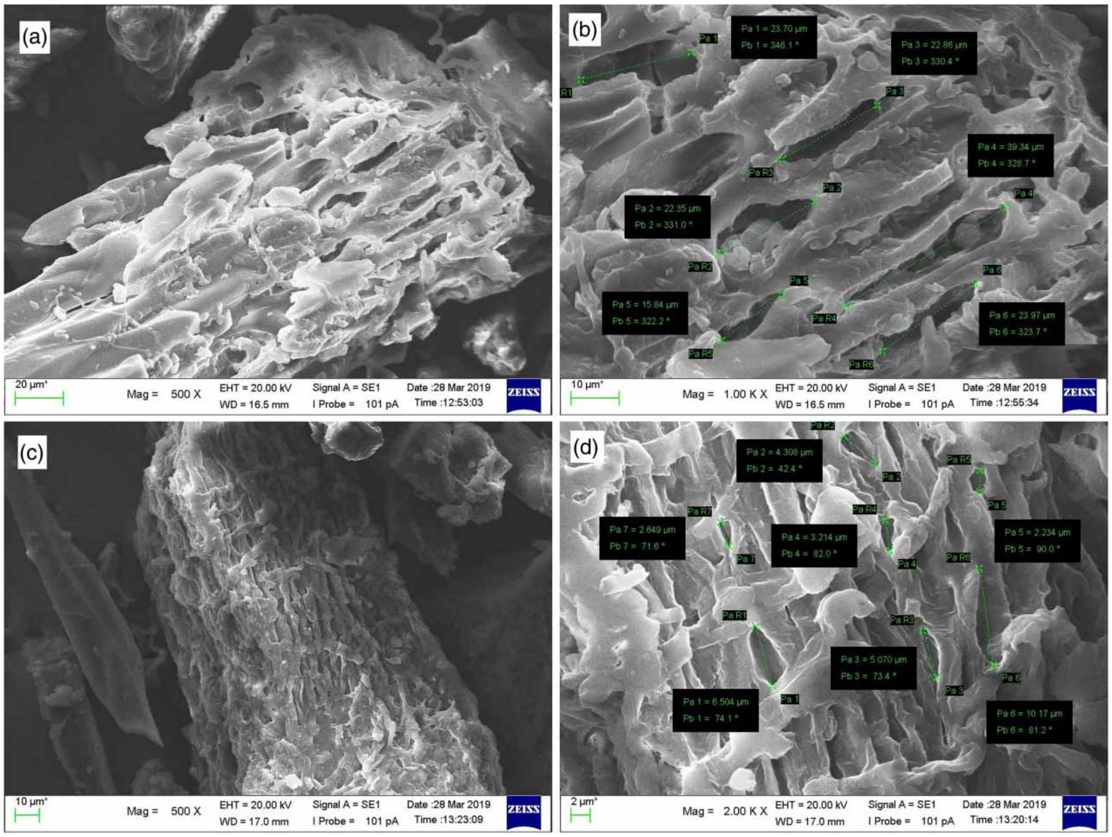

Figure 2 | SEM image of *D. discolor* seed before biosorption at (a) 500X and (b) 1,000X; and after biosorption at (c) 500X and (d) 2,000X.

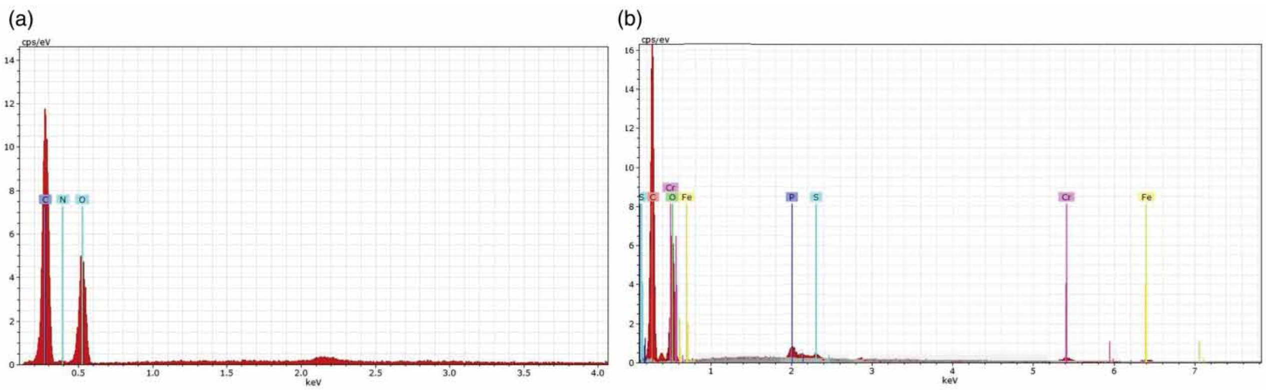

Figure 3 | EDS spectra of *D. discolor* seed before (a) and after (b) biosorption.

at 5.4 keV, whereas the control one showed no peak in this region (Srivastava & Thakur 2012).

The mechanism of adsorption in Cr(VI) was confirmed by FT-IR and EDS analysis. The peak at 3,355.97 cm^{-1} indicated OH groups shifted to the wavenumber of 3,351.89 cm^{-1} after Cr(VI) adsorption. Hydroxyl groups were protonated by nitric acids to $-OH^{2+}/NO^{2-}$. The chemical adsorption process that took place in the adsorbent was anion exchange: $-OH^{2+}/NO^{2-}$ groups became $-OH^{2+}/HCrO^{4-}$ and $-OH^{2+}/CrO_4^{2-}$. Deng *et al.* (2015) and Naushad *et al.* (2017) reported that Cr(VI) adsorption involved physical (electrostatic forces) and chemical (ion exchange) adsorption.

Effect of pH

The effect of pH on the adsorption efficiency of Cr(VI) was studied at five different initial pH levels: 2.50, 3.00, 3.50,

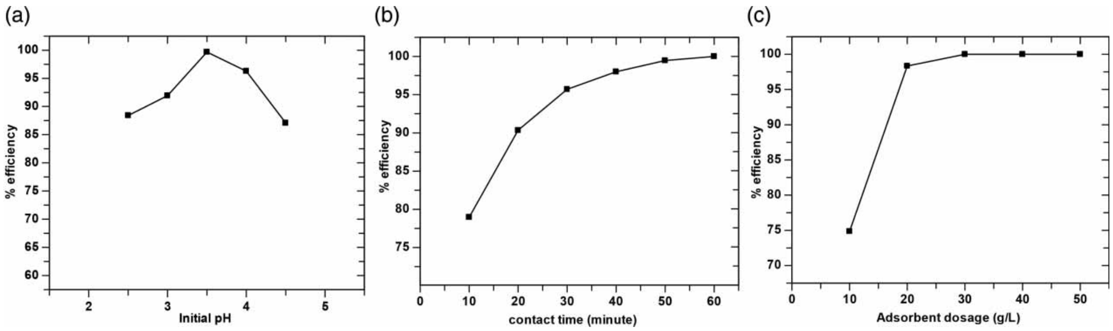

Figure 4 | Effect of (a) pH, (b) contact time and (c) adsorbent dosage on the biosorption efficiency of Cr(VI) ions.

4.00 and 4.50, by keeping all other parameters (contact time, biosorbent dosage and initial Cr(VI) ion concentration) constant, and the results are shown in Figure 4(a). The maximum pH for uptake by adsorbent was 3.50, when the efficiency was 100%. Several other authors have also found that adsorption of Cr(VI) by biomass increases with lower pH, and is highest in the pH range 2–4 (Zein *et al.* 2014; Gogoi *et al.* 2018). The reduction in pH causes the surface of the sorbent to be protonated, but as the pH rises, the concentration of OH^- ions increases the negative charge on that surface (Albadarin *et al.* 2017).

Effect of contact time

The change of Cr(VI) adsorption onto *D. discolor* seed with time is shown in Figure 4(b). After activated *D. discolor* seed was added to the solution, Cr(VI) was rapidly adsorbed and the adsorption efficiency reached 78.97% at 10 min. The adsorption efficiency at 20 min was above 90% and increased continuously to the maximum efficiency of 100% at 60 min. It was deduced that this adsorption was energy independent and that the process was physicochemical (electrostatic forces) (Song *et al.* 2017).

Effect of adsorbent dosage

Biosorption of Cr(VI) by activated *D. discolor* seed was greatly affected by the quantity of biosorbent, as is evident from Figure 4(c). The maximum biosorption of Cr(VI) from the aqueous solution (100%) occurred at a dosage of 30 g/L, beyond which the adsorption efficiency remained unchanged. This might be either because of the saturation of the active sites in *D. discolor* seed or the establishment of the adsorption equilibrium (Saha *et al.* 2017).

A comparison of the maximum percentage removal and adsorption capacity of Cr(VI) onto various biosorbents is shown in Table 1. The maximum percent removal (%E) of *D. discolor* seed was higher than several biosorbents while the maximum adsorption capacity up to 4.4802 mg/g.

Isotherm of biosorption

The initial Cr(VI) concentration was varied from 20–100 mg/L to study the adsorption isotherms. The biosorption data of Cr(VI) on activated *D. discolor* seed was fitted to the Langmuir and Freundlich models (Figure 5). Table 2 summarizes the linear regression data for the Langmuir and Freundlich isotherms for Cr(VI) biosorption using *D. discolor* seed. As indicated in Table 2, the coefficients of determination (R_2) of both models are close to 1. The maximum adsorption capacity (q_m) calculated by the Langmuir model for Cr(VI) was 4.4802 mg/g. The Langmuir isotherm generates a satisfactory fit to the experimental data as indicated by the correlation coefficient. The Langmuir model also seemed to fit well with the experimental data of the Cr(VI) considering the linear regression coefficient was 0.9904.

The Langmuir model assumes that biosorption takes place onto a homogeneous biosorbent surface and that monolayer biosorption occurs on the biosorbent surface

Table 1 | Comparison of maximum percentage removal (%E) and adsorption capacity (q_m) of Cr(VI) on various biosorbents

Biosorbent	(%E)	q_m (mg/g)
Tannery effluent *by Serratia* sp. (Srivastava & Thakur 2012)	75	16.5
Arenga pinnata Merr fruit shell (Zein *et al.* 2014)	41.47	0.52
Cladosporium cladosporioides (Garza-González *et al.* 2017)	51.20	491.85
Eichhornia (Rani *et al.* 2017)	79.20	6.448
Pineapple crown leaf (Gogoi *et al.* 2018)	57.07	12.5
Activated *D. discolor* seed (present study)	100	4.4802

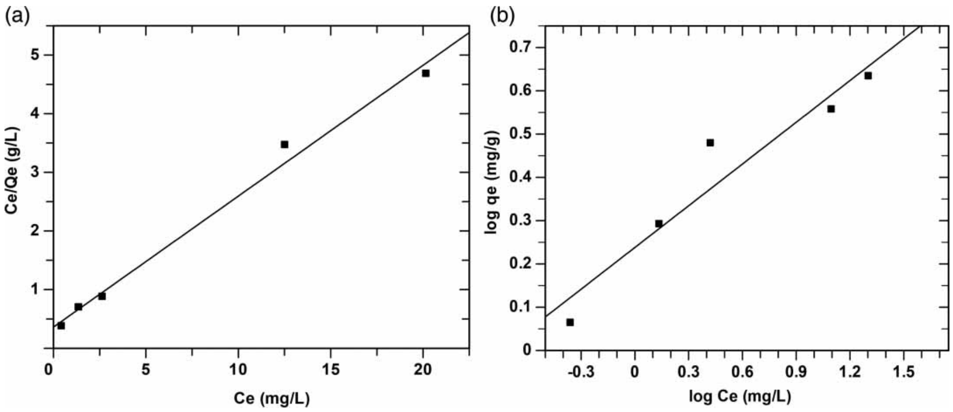

Figure 5 | Biosorption isotherm (pH 3.5, adsorbent dosage 20 g/L) fitted to (a) Langmuir and (b) Freundlich models.

Table 2 | Parameters of isotherm models

Isotherm model	Parameter	Cr(VI)
Langmuir	q_m (mg/g)	4.4802
	b (L/mg)	0.6159
	R^2	0.9904
Freundlich	K_f (L/mg)	1.7314
	n	2.5532
	R^2	0.9229

containing a finite number of identical binding sites (Langmuir 1918). The Freundlich model is entirely an empirical equation, and this model considers the surface heterogeneity of the biosorbent and multilayer biosorption of heavy metal ions onto a heterogeneous surface (Freundlich 1907).

Adsorption kinetics

The pseudo-first-order, pseudo-second-order, and Elovich models were used to model the kinetics of the biosorption process. The experimental data deviated greatly from the fitted curve, indicating the pseudo-first-order kinetics equation (Figure 6(a)) and Elovich equation (Figure 6(c)) were unsuitable to model the adsorption system of activated *D. discolor* seed for Cr(VI). The pseudo-second-order kinetics equation closely described the kinetic process of Cr(VI) adsorption onto activated *D. discolor* seed in terms of the distribution of experimental data on the curve in Figure 6(b). The summaries of the linear equations of the three kinetic models shown in Table 3 also illustrate that the experimental data fit better with the pseudo-second-order kinetics equation than other two models base on the R^2 value (>0.99). According to the pseudo-second-order model, this rate is proportional to the square of the number of empty active sites on the biosorbent (Ho 2006). In the pseudo-first-order kinetic model, the rate of occupation of biosorption sites by the heavy metal ions is proportional to the number of vacant binding sites on the biosorbent (Lagergren 1898). The Elovich model is another rate equation based on biosorption capacity and describes

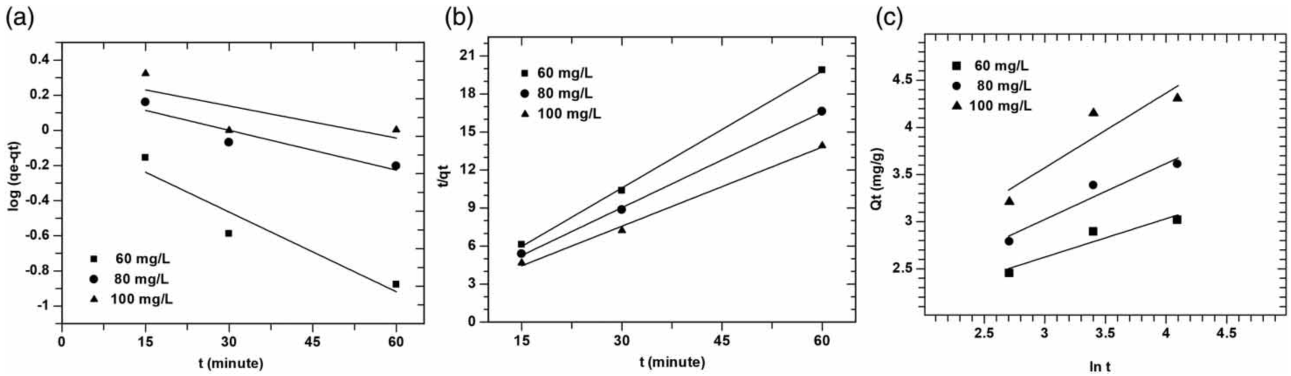

Figure 6 | The pseudo-first-order rate (a), the pseudo-second-order rate (b), and the Elovich model rate (c) for Cr(VI) adsorption by *D. discolor* seed.

Table 3 | Parameters of three kinetic models

	Pseudo-first order			Pseudo-second order			Elovich equation		
C_0 (mg L^{-1})	K_1 (min^{-1})	q_{e1} (mg/g)	R^2	K_2 (g/(mg min))	q_{e2} (mg/g)	R^2	ß (g/mg)	α (mg/(g min))	R^2
60	0.0347	0.987	0.909	0.0695	3.253	0.999	2.4545	12.735	0.905
80	0.0175	1.255	0.886	0.0419	3.985	0.999	1.6857	4.8352	0.936
100	0.0147	1.426	0.747	0.0327	4.803	0.996	1.2631	3.5927	0.855

the kinetics of chemical biosorption onto the heterogeneous biosorbent (Chien & Clayton 1980).

CONCLUSIONS

D. discolor seed effectively removed toxic heavy metal Cr(VI) from aqueous solutions by adsorption. The pH value, the contact time and the biosorbent dosage significantly affected Cr(VI) adsorption onto activated *D. discolor* seed. The maximum adsorption efficiency reached 100% at 60 min, initial pH of 3.5 in 20 g/L adsorbent. The maximum biosorption capacity of the biosorbent was found to be 4.4802 mg/g. The experimental data complied with the Langmuir isotherm model and the pseudo-second-order kinetics equation model. The anion exchange mechanism was confirmed by FT-IR and EDS spectra.

ACKNOWLEDGEMENTS

This research was supported by the research scheme Penelitian Dosen Pemula, from the research fund in the academic year 2017, contract number: 0802/K4/KM/2018 on February 12, 2018, from the Ministry of Research, Technology and Higher Education of the Republic of Indonesia.

REFERENCES

Abdel-Rahman, L. H., Al-Farhan, B. S. F., Abu-Dief, A. M. & Zikry, M. M. 2016 Removal of toxic Pb(II) ions from aqueous solution by nano sized flamboyant pod (*Delonix regia*). *Arch Chem Res.* **1** (1), 3.

Akter, S., Majumder, T., Karim, R. & Ferdous, Z. 2015 Analgesic activities of *Geodorum densiflorum*, *Diospyros blancoi*, *Baccaurea ramiflora* and *Trichosanthes dioica*. *Journal of Pharmacognosy and Phytochemistry* **4** (3), 209–214.

Albadarin, A. B., Collins, M. N., Naushad, M., Shirazian, S., Walker, G. & Mangwandi, C. 2017 Activated lignin–chitosan extruded blends for efficient adsorption of methylene blue. *Chemical Engineering Journal* **307**, 264–272.

Chen, J. P. & Wu, S. N. 2004 Acid/base-treated activated carbons: characterization of functional groups and metal adsorptive properties. *Langmuir* **20**, 2233–2242.

Chien, S. H. & Clayton, W. R. 1980 Application of Elovich equation to the kinetics of phosphate release and sorption in soils. *Soil Science Society of America Journal* **44** (2), 265–268.

Deng, L., Shi, Z. & Peng, X. 2015 Adsorption of Cr(VI) onto magnetic $CoFe_2O_4$/MgAl-LDH composite and mechanism study. *RSC Advances* **5** (61), 49791–49801.

Fomina, M. & Gadd, G. M. 2014 Biosorption: current perspectives on concept, definition and application. *Bioresource Technology* **160**, 3–14.

Freundlich, H. 1907 Über die adsorption in lösungen (About adsorption in solutions). *Zeitschrift für Physikalische Chemie* **57U** (1), 385–470.

Garza-González, M. T., Ramírez-Vázquez, J. E., García-Hernández, M. D. L. Á., Cantú-Cárdenas, M. E., Liñan-Montes, A. & Villarreal-Chiu, J. F. 2017 Reduction of chromium (VI) from aqueous solution by biomass of *Cladosporium cladosporioides*. *Water Science and Technology* **76** (9), 2494–2502.

Gogoi, S., Chakraborty, S. & Saikia, M. D. 2018 Surface modified pineapple crown leaf for adsorption of Cr(VI) and Cr(III) ions from aqueous solution. *Journal of Environmental Chemical Engineering* **6** (2), 2492–2501.

Hausladen, D. M., Alexander-Ozinskas, A., McClain, C. & Fendorf, S. 2018 Hexavalent chromium sources and distribution in California groundwater. *Environmental Science and Technology* **52** (15), 8242–8251.

Ho, Y. S. 2006 Review of second-order models for adsorption systems. *Journal of Hazardous Materials* **136** (3), 681–689.

Howlader, S. I. M., Rahman, M. M., Khalipha, A. B. R., Rahman, M. M. & Ahmed, F. 2012 Antioxidant and antidiarrhoeal potentiality of *Diospyros blancoi*. *International Journal of Pharmacology* **8** (5), 403–409.

Lagergren, S. Y. 1898 Zur Theorie der sogenannten Adsorption gelöster Stoffe, Kungliga Svenska Vetenskapsakademiens (About the theory of so-called adsorption of soluble substances, kungliga svenska vetenskapsakademiens). *Handlingar* **24** (4), 1–39.

Langmuir, I. 1918 The adsorption of gaseson plane surfaces of glass, mica and platinum. *Journal of The American Chemical Society* **40** (9), 1361–1403.

Murungi, J. & Hassanali, A. 2016 Application of chemically modified avocado seed for removal of Copper (II), Lead(II), and Cadmium(II) ions from aqueous solutions. *International Journal of Research in Engineering and Applied Sciences* **6** (8), 1–15.

Naiya, T. K., Singha, B. & Das, S. K. 2011 FTIR study for the Cr (VI) removal from aqueous solution using rice waste. *International Proceedings of Chemical, Biological and Environmental Engineering (IPCBEE)* **10**, 114–119.

Naushad, M., Ahamad, T., Al-Maswari, B. M., Abdullah Alqadami, A. & Alshehri, S. M. 2017 Nickel ferrite bearing nitrogen-doped mesoporous carbon as efficient adsorbent for the removal of highly toxic metal ion from aqueous medium. *Chemical Engineering Journal* **330**, 1351–1360.

Rani, N., Singh, B. & Shimrah, T. 2017 Chromium (VI) removal from aqueous solutions using *Eichhornia* as an adsorbent. *Journal of Water Reuse and Desalination* **7** (4), 461–467.

Saha, G. C., Hoque, M. I. U., Miah, M. A. M., Holze, R., Chowdhury, D. A., Khandaker, S. & Chowdhury, S. 2017 Biosorptive removal of lead from aqueous solutions onto Taro (*Colocasiaesculenta* (L.) Schott) as a low cost bioadsorbent: characterization, equilibria, kinetics and biosorption-mechanism studies. *Journal of Environmental Chemical Engineering* **5** (3), 2151–2162.

Selvaraj, K., Manonmani, S. & Pattabhi, S. 2003 Removal of hexavalent chromium using distillery sludge. *Bioresource Technology* **89** (2), 207–211.

Song, T., Liang, J., Bai, X., Li, Y., Wei, Y., Huang, S., Dong, L., Qu, J. & Jin, Y. 2017 Biosorption of cadmium ions from aqueous solution by modified *Auricularia Auricular* matrix waste. *Journal of Molecular Liquids* **241**, 1023–1031.

Srivastava, S. & Thakur, I. S. 2012 Biosorption and biotransformation of chromium by *Serratia* sp. isolated from tannery effluent. *Environmental Technology* **33** (1), 113–122.

U.S. Environmental Protection Agency 2018 *Edition of the Drinking Water Standards and Health Advisories Tables (EPA 822-F-18-001)*. U.S. Environmental Protection Agency, Washington, DC, USA.

Zein, R., Hidayat, D. A., Elfia, M., Nazarudin, N. & Munaf, E. 2014 Sugar palm *Arenga pinnata* Merr (Magnoliophyta) fruit shell as biomaterial to remove Cr(III), Cr(VI), Cd(II) and Zn(II) from aqueous solution. *Journal of Water Supply: Research and Technology – AQUA* **63** (7), 553–559.

First received 14 January 2019; accepted in revised form 29 March 2019. Available online 9 April 2019